esa

ECOSPHERE

The signature of sea surface temperature anomalies on the dynamics of semiarid grassland productivity

Maosi Chen,[1,]† William J. Parton,[2] Stephen J. Del Grosso,[2,3] Melannie D. Hartman,[1,2] Ken A. Day,[4] Compton J. Tucker,[5] Justin D. Derner,[6] Alan K. Knapp,[7] William K. Smith,[8] Dennis S. Ojima,[2] and Wei Gao[1,2,9]

[1]*United States Department of Agriculture UV-B Monitoring and Research Program, Natural Resource Ecology Laboratory, Colorado State University, Fort Collins, Colorado 80521 USA*
[2]*Natural Resource Ecology Laboratory, Colorado State University, Fort Collins, Colorado 80523 USA*
[3]*Agricultural Research Service, U.S. Department of Agriculture, Fort Collins, Colorado 80526 USA*
[4]*Climate Variability Unit, Science Division, Department of Science, Information Technology and Innovation, Brisbane, Queensland 4001 Australia*
[5]*Earth Resources Branch, NASA/Goddard Space Flight Center, Greenbelt, Maryland 20771 USA*
[6]*United States Department of Agriculture, Agricultural Research Service (USDA-ARS), Rangeland Resources and Systems Research Unit, Cheyenne, Wyoming 82009 USA*
[7]*Department of Biology and Graduate Degree Program in Ecology, Colorado State University, Fort Collins, Colorado 80523-1878 USA*
[8]*School of Natural Resources and the Environment, University of Arizona, Tucson, Arizona 85721 USA*
[9]*Department of Ecosystem Science and Sustainability, Colorado State University, Fort Collins, Colorado 80523 USA*

Citation: Chen, M., W. J. Parton, S. J. Del Grosso, M. D. Hartman, K. A. Day, C. J. Tucker, J. D. Derner, A. K. Knapp, W. K. Smith, D. S. Ojima, and W. Gao. 2017. The signature of sea surface temperature anomalies on the dynamics of semiarid grassland productivity. Ecosphere 8(12):e02069. 10.1002/ecs2.2069

Abstract. We used long-term observations of grassland aboveground net plant production (ANPP, 1939–2016), growing seasonal advanced very-high-resolution radiometer remote sensing normalized difference vegetation index (NDVI) data (1982–2016), and simulations of actual evapotranspiration (1912–2016) to evaluate the impact of Pacific Decadal Oscillation (PDO) and El Niño–Southern Oscillation (ENSO) sea surface temperature (SST) anomalies on a semiarid grassland in northeastern Colorado. Because ANPP was well correlated (R^2 = 0.58) to cumulative April to July actual evapotranspiration (iAET) and cumulative growing season NDVI (iNDVI) was well correlated to iAET and ANPP (R^2 = 0.62 [quadratic model] and 0.59, respectively), we were able to quantify interactions between the long-duration (15–30 yr) PDO temperature cycles and annual-duration ENSO SST phases on ANPP. We found that during cold-phase PDOs, mean ANPP and iNDVI were lower, and the frequency of low ANPP years (drought years) was much higher, compared to warm-phase PDO years. In addition, ANPP, iNDVI, and iAET were highly variable during the cold-phase PDOs. When NINO-3 (ENSO index) values were negative, there was a higher frequency of droughts and lower frequency of wet years regardless of the PDO phase. PDO and NINO-3 anomalies reinforced each other resulting in a high frequency of above-normal iAET (52%) and low frequency of drought (20%) when both PDO and NINO-3 values were positive and the opposite pattern when both PDO and NINO-3 values were negative (24% frequency of above normal and 48% frequency of drought). Precipitation variability and subsequent ANPP dynamics in this grassland were dampened when PDO and NINO-3 SSTs had opposing signs. Thus, primary signatures of these SSTs in this semiarid grassland are (1) increased interannual variability in ANPP during cold-phase PDOs, (2) drought with low ANPP occurring in almost half of those years with negative values of PDO and NINO-3, and (3) high precipitation and ANPP common in years with positive PDO and NINO-3 values.

Key words: aboveground net plant production (ANPP); actual evapotranspiration (AET); advanced very-high-resolution radiometer; Central Plains Experimental Range (CPER); El Niño–Southern Oscillation (ENSO); growing season; normalized difference vegetation index (NDVI); northeastern Colorado; Pacific Decadal Oscillation (PDO); semiarid grassland.

Received 9 June 2017; revised 14 November 2017; accepted 21 November 2017. Corresponding Editor: Laureano A. Gherardi.

† **E-mail:** maosi.chen@colostate.edu

Introduction

Multi-year ocean–atmosphere fluctuations have been linked to North American climate—the Pacific Decadal Oscillation (PDO: after Mantua et al. 1997), which was identified during the 1990s by Mantua et al. (1997), Zhang et al. (1997), and Gershunov and Barnett (1998) referring to the atmospheric component as the North Pacific Oscillation. These multi-year fluctuations in sea surface temperature (SST) involve abrupt basinwide switching in the sign of SST anomalies across the North Pacific. These phase changes occur at approximately 15- to 30-yr intervals for the PDO. El Niño–Southern Oscillation (ENSO) teleconnections with North American climate have different impacts depending on the phase of the PDO (warm or cool; e.g., Hu and Huang 2009, Gershunov and Barnett 1998, Gutzler et al. 2002, McCabe and Dettinger 1999, Wang et al. 2014).

The PDO is referred to as ENSO-like interdecadal variability based on a number of similarities between the ENSO and PDO signals. This includes a weak statistical correlation between the time-series, qualitative similarities in the Pacific-wide SST patterns, and similar impacts on North American climate because of the strength and position of the Aleutian low (Mantua et al. 1997, Zhang et al. 1997, Gershunov and Barnett 1998). Zhu and Liang (2013) have shown that the expansion of the Bermuda High has an impact on strength of the low-level jet in the Great Plains with a strong low-level jet decreasing precipitation in the Southern Great Plains and increasing precipitation in the Northern Great Plains. They also indicate that expansion of the Bermuda High is correlated to the PDO SST. Liang et al. (2015) show that the strength of the low-level jet is correlated to the phase of the El Niño.

Numerous papers (Diaz and Kiladis 1992, Hu and Huang 2009, and Zhu and Liang 2013) have shown that precipitation in the Great Plains is well correlated to PDO/NINO-3 SST patterns. Multi-decadal variations in precipitation in the Southwest United States are correlated to changes in the PDO with increases in precipitation associated with the warm-phase PDO and decreased precipitation associated with cold-phase PDO (McCabe et al. 2004, Hu and Huang 2009). Hu and Huang (2009) show interactive impacts of the PDO and ENSO SST patterns on precipitation in the Southern Great Plains with high precipitation (wet soil conditions) occurring when the ENSO and PDO are both in the positive phase and low precipitation (dry soil conditions) when the ENSO and PDO are both in the negative phases. Note that the ENSO SST changes on a 2- to 4-yr cycle while the PDO index changes on a 15- to 30-yr cycle.

Previous research (Lauenroth 1979, Sala et al. 1988, and Del Grosso et al. 2008) has established that annual precipitation is one of the major factors controlling grassland production in semiarid regions, with aboveground plant production (ANPP) increasing linearly with increasing precipitation at the global, regional, and individual site levels. Irisarri et al. (2016) recently showed that ANPP for a shortgrass steppe in northeastern Colorado at the Central Plains Experimental Range (CPER) decreases linearly with increasing grazing intensity and is highly correlated to spring precipitation (April–June). Research by Hermance et al. (2015) at the CPER site showed that grassland plant growth is most responsive to precipitation in the spring. They also showed that ANPP at the CPER site is highly correlated to integrated growing-season normalized difference vegetation index (iNDVI, cumulative May to September). The Hermance et al. (2015), Irisarri et al. (2016), and Morgan et al. (2016) papers showed that most of the grassland plant production occurs during the April to June time period and that live plant biomass ($R^2 = 0.80$) and ANPP ($R^2 = 0.80$) are highly correlated to iNDVI.

For the semiarid grassland system in Great Plains, there are only limited changes of long-term carrying capacity associated with the long-term moderate and heavy grazing for more

than 70 yr (Milchunas et al. 1994, Porensky et al. 2017). Although the C3 perennial grasses are more responsive to rainfall regimes (Derner et al. 2008), they are not dominant plant functional groups in this ecosystem.

Key for ranchers is the fundamental understanding of knowing whether the mean and variability of forage production differ with the long-term (i.e., 10–20 yr) PDO patterns. This gives ranchers sufficient time for planning, decision-making, and adaptive management. For example, adaptive management can be used to manage complexity associated with precipitation-induced variability in forage production for livestock consumption through incorporating flexibility in animal numbers and grazing season length using science-informed monitoring to help match forage production variability across years and within portions of a grazing season with animal demand (Derner and Augustine 2016). Recent economic models suggest that addition of yearlings to cow–calf operations, for example, provides increased flexibility for ranchers regarding decision-making and profitability in variable climates (Ritten et al. 2010, Torell et al. 2010), especially when stocking decisions are adjusted using available forage and seasonal weather/climate forecasts. Despite the economic advantages of flexible stocking, implementation of this grazing strategy is hindered by limited predictive ability to date regarding accuracy of seasonal weather (3–6 months) forecasting and low-risk approaches of ranchers where the prevailing mantra is to reduce downside risk associated with negative consequences of drought rather than attempting to capitalize on the upside benefits of good years. Thus, the inherently high interannual variability in forage production in these semiarid rangeland ecosystems has resulted in a management approach that is quite conservative with the occurrence of a good year within an unfavorable period of years having little impact on land/grazing management as the emphasis is on recovery of the system from the poor years.

The unique aspect of this paper is the quantification of the impact of the PDO/NINO-3 SSTs on the time-series of three important ecological variables (ANPP, iNDVI, and iAET). This paper will focus on evaluating the impact of PDO and NINO-3 (ENSO index) SST patterns from 1912 to 2016 on cumulative April to July actual evapotranspiration (iAET), ANPP, and iNDVI for the CPER site along with the correlations of iNDVI to ANPP and iAET to ANPP and iNDVI. Morgan et al. (2016) showed that live grassland plant biomass observations are well correlated to NDVI, while Hermance et al. (2015) showed that ANPP is well correlated to iNDVI. We used iAET, rather than rainfall, to correlate to ANPP since it includes the impact of winter precipitation on growing season plant growth (potential storage of soil water during the winter). It was reported that ANPP in western U.S. grasslands is less impacted by growing temperature than precipitation (Mowll et al. 2015). In addition to iAET and precipitation, we also investigated the temperature effects (e.g., April to July mean temperature and cumulative potential evapotranspiration [PET]) on ANPP. The DayCent ecosystem model has a land surface submodel that is capable of simulating daily soil water content, actual evapotranspiration (AET), and plant transpiration in long periods (Parton et al. 1998). Multiple year observations of daily soil water and AET data confirm that the DayCent ecosystem model correctly simulates seasonal changes in soil water and AET at the CPER site.

Site Description and Data Sets

The CPER, a Long-Term Agroecosytem Research network site, is in the precipitation shadow of the Rocky Mountains with annual precipitation of 321 mm (with high inter- and intra-annual variability; Knapp and Smith 2001) and mean annual air temperature of 8.6°C. The site is typical of mid-continental semiarid grasslands with peak precipitation occurring during May and June. The site has a long history of grazing with plant communities dominated by the C4 perennial shortgrass blue grama (*Bouteloua gracilis*) with some C3 perennial graminoids (western wheatgrass (*Pascopyrum smithii*), needle and thread (*Hesperostipa comata*), and threadleaf sedge (*Carex eleocharis*)). Potential plant productivity is highly responsive to spring precipitation amounts (Derner et al. 2008). The data sets used in this analysis include annual estimates of plant production from 1939 to 2016, observed growing season biweekly advanced very-high-resolution radiometer (AVHRR) NDVI (1982–2016), observed

daily maximum and minimum air temperature and precipitation from the CPER site (1912–2016), observed daily soil moisture and AET data (1987–1992, 2001–2003), and observed PDO and ENSO SST anomalies (1912–2016).

ANPP data sets

The ANPP estimates from Lauenroth and Sala (1992) from 1940 to 1990 were derived using a variety of techniques including clipped plots (late July and August) from different sites (4–20) and visual estimates of ANPP. The CPER ANPP estimates from 1983 to 2016 were determined by using the observed live biomass levels from clipped biomass plots (1.8-m^2 quadrants) from three different topoedaphic locations (midslope, ridge, and swale) in a long-term moderately grazed pasture. The sum of clipped live biomass (clipped in late July or early August) from five different plant functional groups (BOBU, CSAG, CSPG, WSPG, and FORB) was used to estimate live grassland plant biomass for each year. The plant functional group BOBU is blue grama plus buffalograss (C4 shortgrasses); CSAG is cool-season annual grasses; CSPG is cool-season perennial graminoids; WSPG is warm-season perennial grasses; and FORB is the combination of annual and perennial forbs. Clipped biomass from shrubs and cactus was excluded in this analysis. The average values of ANPP from 1983 to 2014 were determined by averaging ANPP for the midslope, ridge, and swale topoedaphic locations and are available at (http://hdl.handle.net/10217/81141). A detailed description of how the data were collected is presented by Lauenroth (2013). The CPER ANPP estimates from 1983 to 2014 were used in our detailed statistical climatic analysis because the Lauenroth and Sala (1992) data sets used different techniques (visual and clipped plot estimates of ANPP) over time, and different pastures were used every year (3–30 pastures per year) to determine the average ANPP.

PDO and NINO-3 data sets

The NINO-3 time-series was determined from data published by Physical Sciences Division (2015). The NINO-3 time-series is calculated as the area-weighted average SST anomaly over the central equatorial Pacific (5° S to 5° N, 150° W to 90° W) with the anomaly calculated using a base period of 1951–2000. The specific time-series used is the PSD WG-SP time-series calculated from 1870 to present based on the HADISST 1 data set (Rayner et al. 2003). The PDO time-series was provided by University of Washington, College of the Environment, JISAO (2016; accessed 12/9/2016). The PDO time-series is computed after Mantua et al. (1997) as the leading empirical orthogonal function of North Pacific (20°–70° N) monthly averaged SST anomalies after removing the global mean. The specific time-series is calculated from 1912 to 2016 based on the Reynolds OI SST V2 data set (Reynolds et al. 2007).

AVHRR data set

We used observed AVHRR biweekly values of NDVI measured (NOAA, 1992) for a 3 × 3 pixel array (i.e., average NDVI for 3 × 3 30 m pixels) centered on 104.72943° W and 40.815935° N (Pasture 24 SW section at the CPER site) from 1982 to 2016. We corrected the NDVI values during the growing season by subtracting 0.20 from each value since NDVI values during the non-growing season (November–March) are equal to 0.20 when live plant biomass is minimal. We calculated an integrated growing season NDVI (iNDVI) by cumulating the biweekly NDVI values from May 1 to September 30.

DayCent model description

We used the DayCent model to simulate the annual changes in AET from 1912 to 2016. DayCent (Parton et al. 1998, Del Grosso et al. 2001, 2011) is a biogeochemical model that simulates exchanges of water, carbon, and nutrients (e.g., nitrogen [N]) among the atmosphere, soil, and plants and other ecosystem parameters in response to land management and climate at daily scale. The primary inputs to DayCent include daily weather (maximum and minimum temperatures and precipitation) data, soil texture profile, crop cultivar parameters, crop management practices, and site location (Chen et al. 2016). There are four primary submodels in DayCent: (1) plant growth/productivity, (2) soil organic matter decomposition, (3) land surface, and (4) trace gas (Del Grosso et al. 2001, 2011). We have included a comparison of the DayCent simulated daily AET and soil water with observed soil water and AET data sets from the

CPER site. We used observed daily soil moisture and AET from a three-year Bowen ratio experiment (Parton et al. 2012), observed soil moisture from the NUNN site of Natural Resources Conservation Service (NRCS) from 1996 to 2000 (National Water and Climate Center, NRCS, USDA 2015), and daily lysimeter estimates of AET (Parton et al. 1981) from 1987 to 1992. A detailed description of the DayCent model is found in the online material (Appendix S1).

The weather data required for DayCent including daily maximum and minimum air temperatures and precipitation data (1912_2016) were obtained from multiple sources (Parton et al. 2012, Parton 2013, National Centers for Environmental Information, NOAA 2015, Rangeland Resources Research Unit, ARS. 2015, USDA NRCS [U.S. Department of Agriculture, National Water and Climate Center] 2015). Since there were no weather records at CPER before 1940, weather records between 1912 and 1940 were used from the nearby site at Grover, Colorado. The weather records from these two sites were consolidated in the overlapping period (i.e., 1940–1968). The re-analyzed 3-h solar radiation data between 1979 and 2014 (Physical Sciences Division, ESRL, NOAA 2015) were accumulated at daily scale as an extended weather input. In addition, these data were used to calibrate the twelve solar radiation monthly adjustment coefficients for correct daily solar radiation estimation from daily temperatures before 1979.

Statistical analysis of data

The annual changes in April–July cumulative AET from 1912 to 2016 were correlated to the changes in the warm- and cold-phase PDO patterns (three warm phases and three cold phases) and annual average April–June PDO and NINO-3 SST anomalies. We determined the impact of the PDO and NINO-3 anomalies on the frequency of low (tercile 1), medium (tercile 2), and high (tercile 3) AET years. We used the observed CPER ANPP data (1983 to 2014) to determine the correlation of annual ANPP to cumulative April–July AET and iNDVI.

Multiple regression analysis was used to determine the potential impact of April–July cumulative potential evapotranspiration (iPET) and mean air temperature (TEMP) in addition to iAET on ANPP.

The term variability in this paper refers to a quantity's degree of being changeable in a given time window. It is defined as follows:

$$\text{Variability} = \frac{\sum_{t=1}^{T-1} abs(y_{t+1} - y_t)}{T-1} \quad (1)$$

where the term y refers to the quantity of interests; the subscripts refer to the time points; the number of total time points is T; and the term *abs ()* refers to the absolute operator. In this paper, the variability is calculated for April–July cumulative AET (iAET), cumulative May–September NDVI (iNDVI), and the annual observed aboveground plant productivity (ANPP) during the warm- and cold-phase PDOs.

Results

DayCent model evaluation

The DayCent model was used to simulate daily soil water and AET from 1912 to 2016 for the CPER site. The ability of the model to simulate plant ecosystem dynamics for the CPER site (seasonal live leaf dynamics and net ecosystem carbon exchange) has been documented by Chen et al. (2016) using observed live leaf biomass and net carbon exchange data from a three-year eddy covariance data set (2001–2003). We used the observed daily AET data from Parton et al. (2012) and daily AET data (1987–1992) from a lysimeter located at the CPER site (Parton et al. 1981) to test model performance. The results show that modeled AET is highly correlated with observed daily, weekly, and monthly AET (R^2 = 0.55, 0.81, and 0.92, respectively; Appendix S2). DayCent simulated vs. observed seasonal patterns in AET and soil water are presented in the online material (Appendices S3, S4). The results show that maximum AET rates and soil water contents are observed during the May to June season and that AET rates and soil water content are higher, and decrease with time, following the rainfall events. These observed changes in AET and soil water content following rainfall events are well simulated by DayCent, indicating the suitability of the model to simulate changes in AET from 1912 to 2016.

As expected, we found that ANPP (1983–2014) was well correlated to iNDVI (R^2 = 0.59) and that ANPP was highly correlated (R^2 = 0.58) to iAET for the same time period. We also found

that iAET was positively correlated to iNDVI (quadratic model, $R^2 = 0.62$). These results show the strong autocorrelation among iAET, iNDVI, and ANPP.

We found that iAET and cumulative April to July precipitation (iPREC) have similar correlations with ANPP. It is expected since iAET and iPREC have a high correlation ($R^2 = 0.88$ excluding two extreme points where iPREC exceeded iAET and one point where iAET is significantly higher than iPREC because of snow water storage in the winter). In addition, we found that on average iAET exceeded iPREC by 1–3 cm on an annual basis. The higher iAET values compared to iPREC are the results of a net storage of 1.6 cm of water during the November 1 to March 31 time period. The ratio of iPREC to iAET shows that 85.3% of the time the ratio is <1.05, indicating that most of the precipitation falling during the April to July time period is last due to evapotranspiration. Our results also show that daily PET during the April to July time period is greater than daily AET and precipitation 84.1% of the time.

The regression analysis correlated ANPP to iAET and iPET, and TEMP. The results show including the iPET and TEMP variables in the ANPP multiple regression analysis does not improve the R^2 (all around 0.58) between iAET to ANPP. The results also show that correlating the ratio of iAET and iPET to annual ANPP has the similar correlation (i.e., $R^2 = 0.59$) as iAET to ANPP.

PDO/NINO correlations with iAET, iNDVI, and ANPP

The primary objective of this paper is to document the correlations of the PDO and NINO-3 SST anomalies to ANPP, iNDVI, and iAET at the CPER site. Fig. 1 shows the changes in the PDO (Fig. 1A) and NINO-3 (Fig. 1B) anomalies from 1912 to 2016. The data show 15- to 30-yr time periods with either above-normal or below-normal SST anomalies for PDOs, which include three cold phases (1912–1924, 1945–1977, and 1999–2013) and three warm phases (1925–1944, 1978–1998, and 2014–2016). The NINO-3 (ENSO SST patterns) sea surface anomalies vary with a much higher frequency (1- to 3-yr pattern) and NINO-3 has a weak positive correlation to PDO ($R^2 = 0.20$). The historical changes in growing season temperature (April–October; Fig. 1C) show a general trend for increasing temperatures during the whole time period; however, growing season temperatures are higher during the warm-phase PDOs. This pattern is demonstrated with the 1978–1997 warm phase that has higher temperatures compared to the subsequent 1998–2013 cold-phase PDO (mean temperatures of 16.2°C for the warm phase and 15.0°C for the cold phase).

The DayCent simulated changes in iAET from 1912 to 2016 (Fig. 1D) show large year-to-year variability in iAET with higher variability in iAET during cold-phase PDOs compared to the warm-phase PDOs (Appendix S5: Table S1). Most of the high iAET rates (>26 cm/yr) and low iAET rates (<16 cm/yr) occurred during the cool-phase PDOs (72.0% of the high rates and 63.2% of the low iAET rates for cold-phase PDOs between 1912 and 2016). This pattern is quite strong during the 1998–2013 cold-phase PDO period with large negative year-to-year changes in iAET (i.e., droughts followed by wet years for much of the time). Comparison of the observed plant production from 1939 to 2014 with the iAET data (Fig. 1D, E) shows a high correlation of ANPP to iAET ($R^2 = 0.45$ excluding four extreme points; 1942, 1943, 1981, and 2009) with the high year-to-year variability in ANPP primarily resulting from yearly changes in iAET. Comparison of the mean ANPP during the cold- and warm-phase PDO show that ANPP is lower during the cold-phase PDOs (ANPP = 65.0 g (dry mass)/m^2 during the cold-phase PDOs vs. 86.1 g (dry mass)/m^2 during the warm-phase PDOs). The results show that vast majority of the low ANPP values (<40 g (dry mass)/m^2) occur during the cold-phase PDOs (100% between 1939 and 2016).

Fig. 2 shows the frequency distributions of iAET, iNDVI, and ANPP in terms of the cold and warm PDO phases. It is seen that in warm-phase PDOs iAET has a narrower normal-like distribution than in cold PDO periods, but their mean values are close, which is consistent with Table 1. For example, the low-iAET years (i.e., iAET < 15 cm) are more frequent during the cold-phase PDOs (17%) than in the warm-phase PDOs (11%). Similarly, the high-iAET years (i.e., iAET > 25 cm) are also more frequent during the cold-phase PDOs (35%) than in the warm-phase PDOs (20%). In

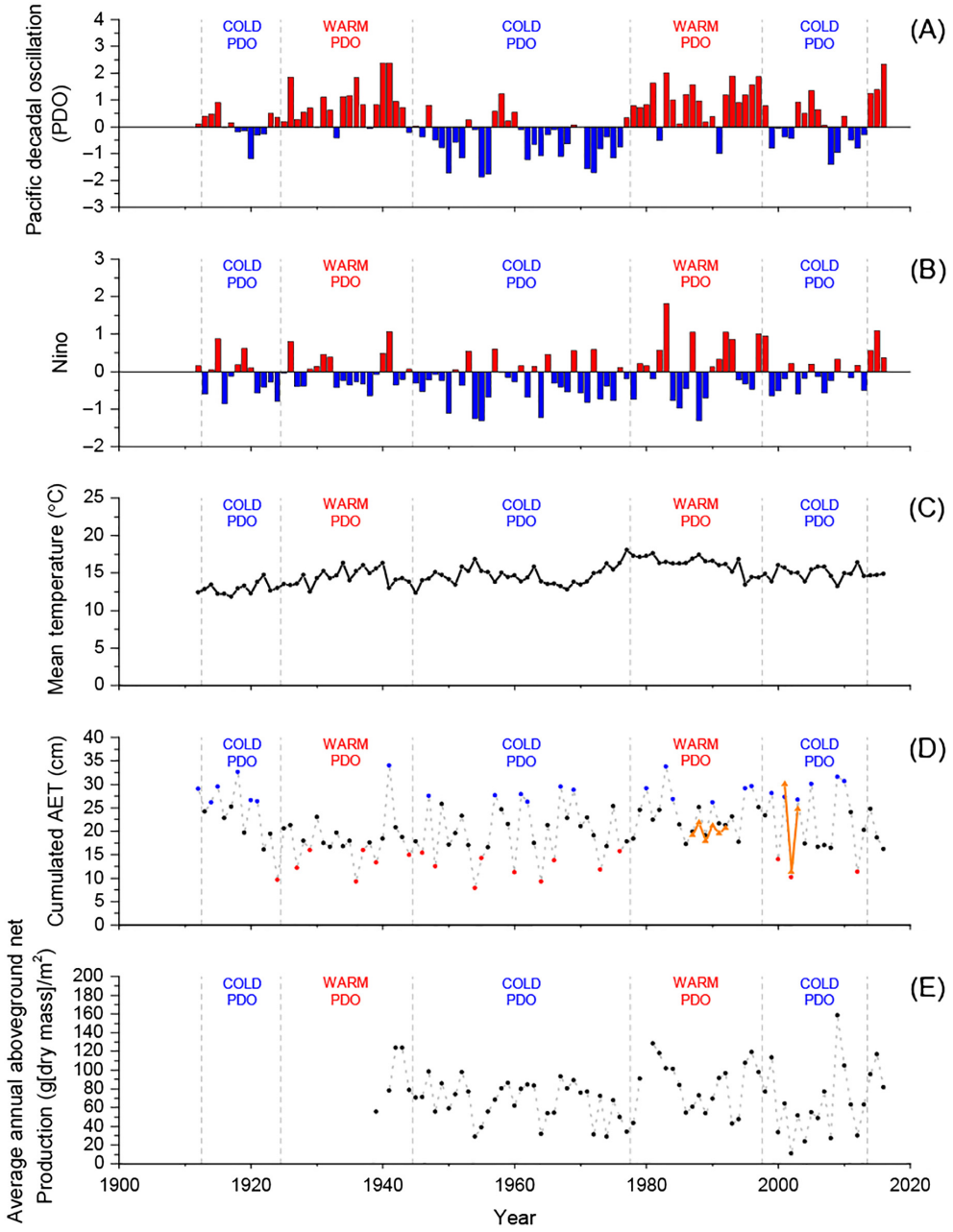

Fig. 1. Average April to June Pacific Decadal Oscillation (A) and NINO3 (B) sea surface temperature anomalies from 1912 to 2016, average growing season (April–October) air temperatures (C), DayCent simulated cumulative actual evapotranspiration rates from 1912 to 2016 (red points: iAET < 16 cm/yr; blue points: iAET > 26 cm/yr) as well as observed iAET from 1987 to 1992 and from 2001 to 2003 (yellow dots and lines; D), and observed aboveground plant production (ANPP) for the Central Plains Experimental Range (CPER) site from 1939 to 2016 (E). The ANPP data from Lauenroth and Sala (1992) were used from 1939 to 1990, while the observed ANPP from the CPER site was used from 1983 to 2016.

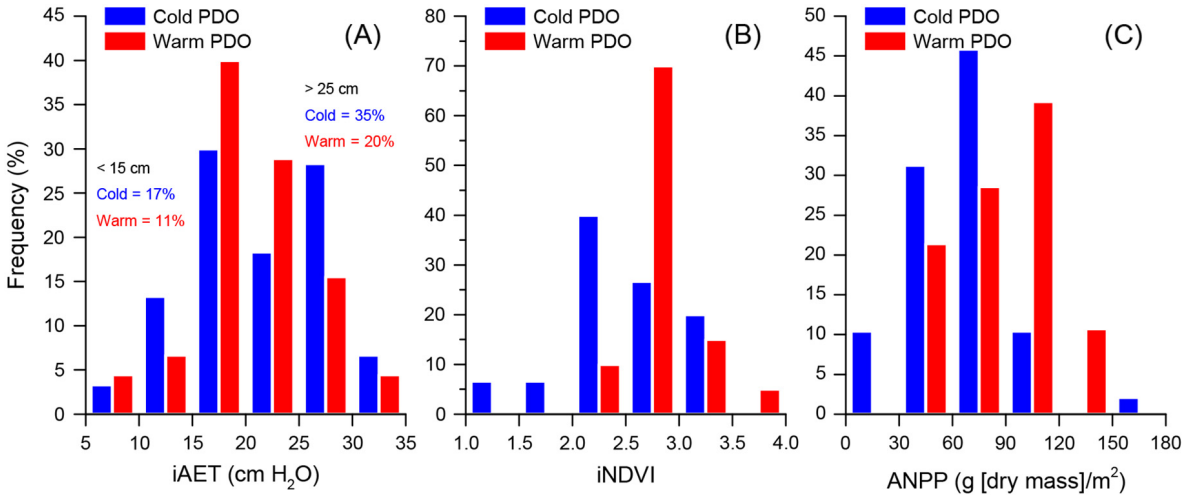

Fig. 2. The frequency distribution of iAET between 1912 and 2016 (A), iNDVI between 1982 and 2016 (B), and ANPP between 1939 and 2016 (C) in terms of the cold and warm Pacific Decadal Oscillation (PDO) periods.

contrast, the frequency distributions of iNDVI and ANPP during the warm-phase PDOs show an obvious positive shift from the corresponding distribution during the cold-phase PDOs.

The impact of annual values of PDO and NINO-3 anomalies on the frequency of low (tercile 1), medium (tercile 2), and high (tercile 3) iAET years is shown in Fig. 3. Fig. 3A shows the distribution of low, medium, and high iAET years as a function of the April to June average PDO and NINO-3 anomalies. PDO and NINO-3 values are positively correlated (R^2 = 0.20), most of the low-iAET years (purple diamonds) occur when both PDO and NINO-3 are negative

Table 1. Mean and variability of the cumulative (April to July) actual evapotranspiration rates (iAET), observed aboveground plant production (ANPP), cumulative NDVI (iNDVI—May to September), and the number and frequency of drought years (AET <14 cm (H_2O)/yr) and low plant production years (<40 g (biomass)·m^{-2}·yr^{-1}) for the different cold and warm PDO periods from 1924 to 2016.†

Variable	PDO period	Variability‡	Mean‡	Number (Frequency, %) of drought years	Number (Frequency, %) of low ANPP years
April–July AET	WARM (1924–1944)	5.508	17.70	4 (19.0)	N/A
April–July AET	COLD (1945–1977)	7.462	19.60	6 (18.2)	N/A
April–July AET	WARM (1978–1998)	4.815	23.78	0 (0.0)	N/A
April–July AET	COLD (1999–2013)	10.087	21.43	2 (13.3)	N/A
April–July AET	WARM (2014–2016)	N/A	19.87	N/A	N/A
Aboveground plant productivity	COLD (1945–1977)	21.491	66.51	N/A	6 (18.2)
Aboveground plant productivity	WARM (1978–1998)	21.530	82.88	N/A	0 (0.0)
Aboveground plant productivity	COLD (1999–2013)	45.641	61.61	N/A	5 (33.3)
Aboveground plant productivity	WARM (2014–2016)	N/A	97.92	N/A	N/A
Cumulated NDVI	WARM (1982–1998)	0.248	2.70	N/A	N/A
Cumulated NDVI	COLD (1999–2013)	0.657	2.46	N/A	N/A
Cumulated NDVI	WARM (2014–2016)	N/A	3.19	N/A	N/A

Note: NDVI, normalized difference vegetation index; PDO, Pacific Decadal Oscillation.

† Only mean values of iAET, ANPP, and iNDVI are presented for the 2014 to 2016 warm PDO because there are only three years of data.

‡ The unit of variability and mean depends on the variable. For April to July AET, the unit is cm (H_2O)/year; for aboveground plant productivity, the unit is g (biomass)·m^{-2}·yr^{-1}; for cumulated NDVI, the unit is 1/yr.

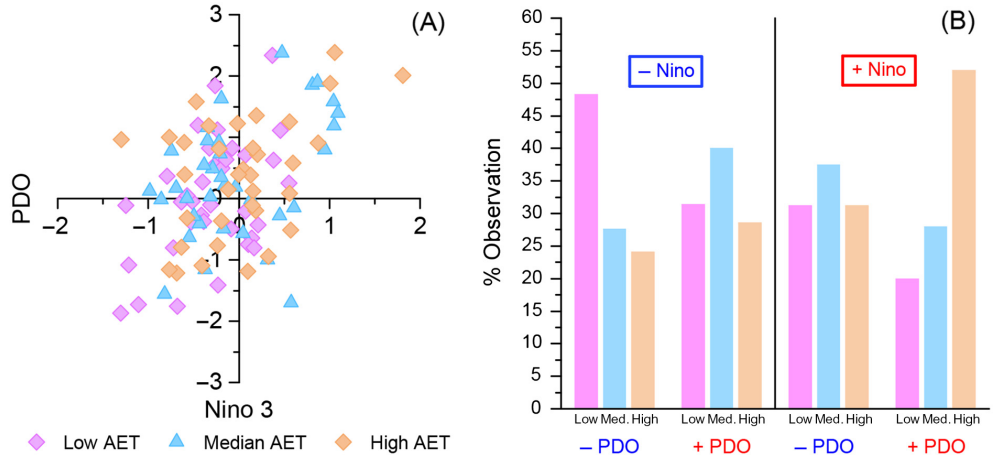

Fig. 3. Distribution of low, medium, and high actual evapotranspiration (AET) years as a function of the April–June Pacific Decadal Oscillation (PDO) and NINO-3 anomalies (A) and the relative frequency of low, medium, and high AET years (B) as a function the four PDO/NINO-3 phases (positive PDO and NINO-3, negative PDO and NINO-3, negative PDO and positive NINO-3, and positive PDO and negative NINO-3). Low AET years include the years with the lowest AET values (33% of the observations). Average AET years are the 33% in the middle, and high AET years include the 33% of the years with the highest AET values from 1912 to 2016.

values, and there is a high frequency for high iAET years (yellow diamonds) when PDO and NINO-3 both have positive values. The frequency distribution for low, medium, and high iAET years (Fig. 3B) as a function of PDO/NINO-3 phases (positive PDO and NINO-3, negative PDO and NINO-3, negative PDO and positive NINO-3, and positive PDO and negative NINO-3) shows that for positive NINO-3 yr (either negative or positive PDO) drought frequency is low (low iAET years, pink bars) with a higher frequency for wet years (high iAET years, light yellow bars). If both PDO and NINO-3 are positive, this pattern of low frequency for droughts (about 20%) and a high probability for a wet year (about 52%) is enhanced. The years when NINO-3 is negative show a general pattern of high frequency of drought (dry years) and a low frequency of a wet year. The results for both cold and warm NINO-3 values show that when PDO values increase from negative to positive values, there is a decrease in the frequency of low iAET and an increase in the frequency of high iAET. These results suggest that PDO SSTs modulate the impact of NINO-3 (ENSO) on the frequency of low and high iAET years with little change in the frequency of low, medium, and high iAET years when PDO and NINO-3 SSTs are in opposite phases.

Morgan et al. (2016) showed that MODIS-derived NDVI values at the CPER site are highly correlated to the live biomass (R^2 = 0.90 for seasonal patterns in live biomass vs. pasture NDVI during 2001–2003). We used the observed cumulative growing season NDVI (iNDVI, May to September) as an index of live biomass and plotted iNDVI changes from 1982 to 2016 (Fig. 4A). The results show that iNDVI values are higher and less variable during the 1977–1998 warm-phase PDO compared to the values for the most recent 1999–2013 cold-phase PDO (Table 1). Fig. 4B shows the seasonal average NDVI patterns for 1999–2013 cold-phase PDO and the 1982–1998 warm-phase PDO along with the standard deviations. The results show that average NDVI values (live plant biomass) increase rapidly from April to June and decrease from July until the end of October. The results show very low standard deviations in May and June NDVI values for the warm-phase PDO and very high standard deviation for the cold-phase PDO. The high standard deviations for the cold-phase PDO result from the frequent droughts and low plant production observed during the cold-phase PDO (low plant production and droughts in 2000, 2002, 2004, 2006, and 2012).

Table 1 presents a summary of the impact of cold- and warm-phase PDOs (1924–2016) on

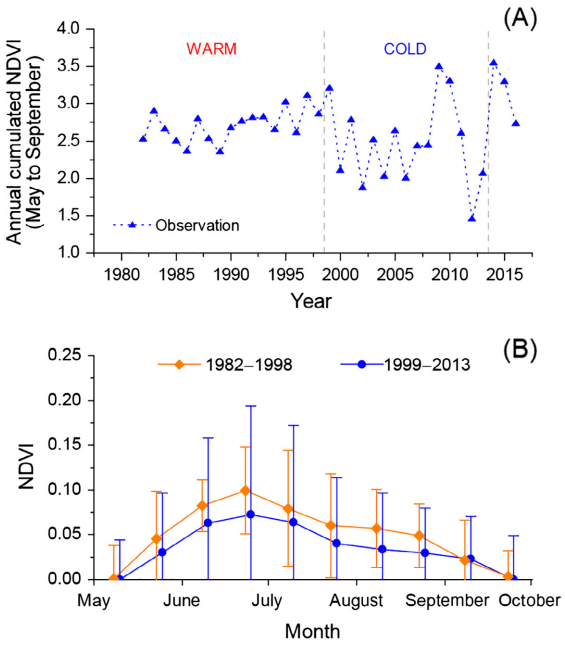

Fig. 4. Observed growing season cumulative (April–October) advanced very-high-resolution radiometer-derived normalized difference vegetation index (NDVI) from 1982 to 2016 (A) and seasonal patterns of the average NDVI and standard deviation of NDVI for the cold-phase Pacific Decadal Oscillation (PDO; 1999–2013) and the warm-phase PDO (1982–1998; B). A shift of −0.2 is applied to all values in panel (B) to highlight the NDVI variability during the cold- and warm-phase PDOs.

mean and variability of iAET, iNDVI, and ANPP. The results show a consistent pattern of high variability and lower mean iNDVI and ANPP for the cold-phase PDO, while the iAET data show a consistent pattern of higher variability during the cold phase. The PDOs with the highest variability in iNDVI, iAET, and ANPP all occurred during the most recent cold-phase (1998–2013) PDO. Table 1 also presents the number and frequency of droughts (<14 cm iAET) and low plant production years (<40 g (dry mass)/m^2) for the cold- and warm-phase PDOs with a consistent pattern of high drought frequency and low plant production for the cold-phase PDOs.

Discussion

The main goal of this paper was to evaluate the impact of SST anomalies (PDO and NINO-3) on the dynamics of semiarid grassland productivity at the CPER site in northeastern Colorado. The results from Table 1, Figs. 1–3 show a clear pattern of high variability in live plant biomass (iNDVI), ANPP, and iAET during the cold-phase PDOs as well as higher frequency of low plant production and droughts. The annual PDO and NINO-3 SST results show that iAET is high when PDO and NINO-3 SST values are positive while negative values of PDO and NINO-3 are associated with low iAET. The strong interactive impact PDO and NINO-3 on iAET is shown by the pattern of highest frequency of above-normal iAET and lowest frequency of below-normal iAET when PDO and NINO-3 are positive, the opposite pattern when PDO and NINO-3 are both negative, and results showing similar frequency of low and high iAET years when PDO and NINO-3 SSTs are in the opposite phases. Our results are consistent with observations from Hu and Huang (2009) and McCabe et al. (2004), which show high drought frequency in the Southwest United States for the cold-phase PDO and low drought frequency for the warm-phase PDO. These results are also consistent with observations of Hu and Huang (2009), which show strong interactive impacts of the PDO and NINO-3 SSTs on precipitation, that is, high precipitation (wet soil conditions) occurring when the NINO-3 and PDO are both in the positive phase and low precipitation (dry soil conditions) when the NINO-3 and PDO are both in the negative phases. Our results are similar to those presented by Power et al. (2006) for rainfall in Australia showing a strong interactive impact of ENSO and PDO on rainfall patterns in Australia. The opposite patterns (compared to the CPER site) are observed in Australia with high precipitation observed when PDO and NINO-3 are both negative and low precipitation observed when PDO and NINO-3 are both positive.

Many authors (Lauenroth 1979, Sala et al. 1988, Lauenroth et al. 1999) have evaluated the impact of annual and growing season precipitation on ANPP and generally found that grassland ANPP increases linearly with increasing precipitation. Our results show a strong linear correlation (R^2 = 0.58) of ANPP to iAET. A recent paper by Morgan et al. (2016) showed that April to June AET and precipitation-controlled annual growing season net carbon uptake for the CPER

site, while Derner and Hart (2007) showed that cumulative April to June rainfall is highly correlated to ANPP for a nearby grassland site in Cheyenne, Wyoming. Morgan et al. (2016) and Derner and Hart (2007) suggested that the July and August precipitation have little impact on ANPP. Furthermore, Hermance et al. (2015) also showed that the precipitation at the end of the growing season has little impact on plant growth.

The results show that ANPP is well correlated to both iAET and iPREC. This is primarily a result of the high autocorrelation of iAET to iPREC (R^2 = 0.88) with annual AET values generally 1–3 cm higher than precipitation. The higher AET values compared to precipitation are a result of average net storage of 1.6 cm of water during the winter time period (November 1–March 31). The fact that ratio of iPREC to iAET is <1.05 85.3% of the time shows that the vast majority of the precipitation falling during the April to July time period is lost as evapotranspiration. This is a result of the fact that daily PET exceeds rainfall and AET 84.1% of the time at CPER site. These results are consistent with other papers from dry grasslands in the western part of the Great Plains where PET rates are much greater than precipitation inputs (Yang et al. 1998, Lauenroth and Bradford 2006, Knapp et al. 2008).

We attempted to determine whether iPET and TEMP have any impact on annual ANPP using regression analysis. The results show that including TEMP and iPET in the regression of iAET to ANPP does not improve the correlation of AET to ANPP and thus suggest that rainfall (highly correlated to iAET) is the most important variable controlling grassland plant production at CPER site. These results are consistent with a recent paper (Mowll et al. 2015) showing that rainfall is the primary control on grassland plant production and that adding temperature had a relatively small impact on improving the correlation of rainfall to ANPP for Great Plains grasslands. The results from the Mowll et al. (2015) paper showed that mean growing season temperature was negatively correlated to ANPP and suggested that using existing ANPP data sets to predict the future impact of increases in temperature associated with potential climatic changes is difficult as warming can have either positive or negative effects depending the ratio of C3/C4 grasses in the plant community.

We used extensive observed daily soil water and AET data sets (9 yr of AET data and 6 yr of soil water data) from the CPER site to test the ability of the DayCent model to simulate daily soil water dynamics and AET rates at the site. The results show that the model accurately simulated daily, weekly, and monthly AET rates with R^2 values for the observed vs. simulated AET rates increasing from 0.55 for daily values to 0.92 for monthly values. Comparison of observed vs. simulated soil water dynamics (Appendix S4) showed that the model accurately simulated the seasonal changes in soil water content and the daily changes in soil water following rainfall events (decreasing with time). The DayCent model has successfully been used to simulate soil water and AET dynamics for grassland, agricultural, and forest systems (Parton et al. 1998, Savage et al. 2013, Scheer et al. 2014, Hudiburg et al. 2015, Chen et al. 2016).

Correlation of growing season cumulative NDVI (iNDVI) with observed plant production at the CPER site shows a high correlation of iNDVI to ANPP (R^2 = 0.59). As expected, the correlation of iNDVI to iAET is high (quadratic model, R^2 = 0.62) along with the correlation of ANPP to cumulative iAET. These results suggest the potential to use iNDVI values for grasslands in the U.S. Great Plains to determine the yearly changes in ANPP using AVHRR-derived NDVI data sets. Advanced very-high-resolution radiometer seasonal NDVI data are currently available at the global scale (5 × 5 km grid) from 1982 to the present time (Smith et al. 2016) and could be used to project yearly changes in ANPP for Great Plains grassland using regionally calibrated correlation of ANPP to iNDVI. The Hermance et al. (2015) paper also shows the potential to use iNDVI to determine ANPP with a strong correlation of ANPP to MODIS iNDVI (R^2 = 0.75). The Gilmanov et al. (2005) and Zhang et al. (2010) papers also show the strong correlations of NDVI to plant production and net growing season carbon uptake for grasslands in the Great Plains.

The PDO pattern recently (2013) changed from the cold phase to the warm phase. A simple extrapolation of the historical patterns from the last 100 yr would suggest ANPP and iAET will

be higher and less variable at the CPER site during the next 15–20 yr. The recent ANPP data (2014–2016) show high plant production, which is consistent with historical patterns for warm-phase PDOs. Knowledge of these patterns has important implications to rangeland and especially for adaptive grazing management (Derner and Augustine 2016) by ranchers in this semiarid grassland ecosystem. Understanding that the warm-phase PDO is likely to result in higher average, and less variable, ANPP for next decade plus provides opportunities for ranchers to revise short- and long-term planning efforts, and enhance decision-making related to adaptive grazing management by more effectively matching animal demand with forage availability. It is unclear how potential long-term changes in the climate will impact ANPP patterns since the observed data for the last cold-phase PDO (1999–2013) showed that ANPP and iAET had the highest variability during the historical record. During this prior cold-phase PDO, the highly variable ANPP resulted in ranchers in this ecosystem having to make reactive decisions related to purchasing feed/hay, finding additional pastures, and/or selling livestock during the dry years (Kachergis et al. 2014).

Conclusions

The key results from this study show that yearly changes in aboveground plant production, iNDVI (index of growing season live biomass), and April–July cumulative AET (highly correlated to ANPP) are altered by the PDO and NINO-3 SST patterns. ANPP, iNDVI, and iAET values are much more variable during the cold-phase PDO periods compared to the warm-phase PDO. This high variability we attribute to a high frequency for droughts and low plant production years during the cold-phase PDO years, as evidenced by low average annual ANPP and iNDVI values for these years. Annual ANPP is well correlated to iNDVI and iAET, and there is strong autocorrelation among all of these ecosystem variables. There is a strong impact of PDO and NINO-3 SST patterns on iAET with positive values of PDO and NINO-3 (ENSO index) causing increases in precipitation and negative values of PDO and NINO-3 causing decreases in precipitation.

Acknowledgments

Support for this research came from the U.S. Department of Agriculture (USDA) UV-B Monitoring and Research Program (Grants 2015-34263-24070 and 2016-34263-25763), the USDA cooperative agreements (Grants 58-5402-4-001, 59-1902-4-00), and the USDA National Institute of Food and Agriculture (NIFA) project (2015-67003-23456).

Literature Cited

Chen, M., W. J. Parton, E. C. Adair, S. Asao, M. D. Hartman, and W. Gao. 2016. Simulation of the effects of photodecay on long-term litter decay using DayCent. Ecosphere 12:e01631-1–e01631-22.

Del Grosso, S. J., W. J. Parton, C. A. Keough, and M. Reyes-Fox. 2011. Special features of the DayCent modeling package and additional procedures for parameterization, calibration, validation, and applications. Pages 155–176 *in* L. R. Ahuja and L. Ma, editors. Methods of introducing system models into agricultural research. American Society of Agronomy, Madison, Wisconsin, USA.

Del Grosso, S. J., W. J. Parton, A. R. Mosier, M. D. Hartman, J. Brenner, D. S. Ojima, D. S. Schimel. 2001. Simulated interaction of carbon dynamics and nitrogen trace gas fluxes using the DAYCENT model. Pages 303–332 *in* M. Schaffer, et al., editors. Modeling carbon and nitrogen dynamics for soil management. CRC Press, Boca Raton, Florida, USA.

Del Grosso, S. J., W. J. Parton, T. S. Stohlgren, D. Zheng, D. Bachelet, S. Prince, K. Hibbard, and R. Olson. 2008. Global potential net primary production predicted from vegetation class, precipitation, and temperature. Ecology 89:2117–2126.

Derner, J. D., and D. J. Augustine. 2016. Adaptive management for drought on rangelands. Rangelands 38:211–215.

Derner, J. D., and R. H. Hart. 2007. Grazing-induced modifications to peak standing crop in northern mixed-grass prairie. Rangeland Ecology & Management 60:270–276.

Derner, J. D., B. W. Hess, R. A. Olson, and G. E. Schuman. 2008. Functional group and species responses to precipitation in three semi-arid rangeland ecosystems. Arid Land Research and Management 22:81–92.

Diaz, H. F., and G. N. Kiladis. 1992. Atmospheric teleconnections associated with the extreme phases of the Southern Oscillation. Pages 7–28 *in* H. F. Diaz and V. Markgraf, editors. El Niño: Historical and Paleoclimatic Aspects of the Southern Oscillation.

Cambridge University Press, New York, New York, USA.

Gershunov, A., and T. P. Barnett. 1998. Interdecadal modulation of ENSO teleconnections. Bulletin of the American Meteorological Society 79:2715–2725.

Gilmanov, T. G., L. L. Tiezen, B. K. Wylie, L. B. Flanagan, A. B. Frank, M. R. Haferkamp, T. P. Myers, and J. A. Morgan. 2005. Integration of CO2 flux and remotely-sensed data for primary production and ecosystem respiration analyses in the Northern Great Plains: potential for quantitative spatial extrapolation. Global Ecology and Biogeography 14:271–292.

Gutzler, D. S., D. M. Kann, and C. Thornbrugh. 2002. Modulation of ENSO-based long-lead outlooks of southwestern US winter precipitation by the Pacific Decadal Oscillation. Weather and Forecasting 17:1163–1172.

Hermance, J. F., D. J. Augustine, and J. D. Derner. 2015. Quantifying characteristic growth dynamics in a semi-arid grassland ecosystem by predicting short-term NDVI phenology from daily rainfall: a simple four parameter coupled-reservoir model. International Journal of Remote Sensing 36:5637–5663.

Hu, Z., and B. Huang. 2009. Interferential impact of ENSO and PDO on dry and wet conditions in the US Great Plains. Journal of Climate 22:6047–6065.

Hudiburg, T. W., S. C. Davis, W. Parton, and E. H. DeLucia. 2015. Bioenergy crop greenhouse gas mitigation potential under a range of management practices. Global Change Biology – Bioenergy 7:366–374.

Irisarri, J. G. N., J. D. Derner, L. M. Porensky, D. J. Augustine, J. L. Reeves, and K. E. Mueller. 2016. Grazing intensity differentially regulates ANPP response to precipitation in North American semiarid grasslands. Ecological Applications 26:1370–1380.

Kachergis, E., J. D. Derner, B. B. Cutts, L. M. Roche, V. T. Eviner, M. N. Lubell, and K. W. Tate. 2014. Increasing flexibility in rangeland management during drought. Ecosphere 5:1–14.

Knapp, A. K., and M. D. Smith. 2001. Variation among biomes in temporal dynamics of aboveground primary production. Science 291:481–484.

Knapp, A. K., et al. 2008. Shrub encroachment in North American grasslands: Shifts in growth form dominance rapidly alters control of ecosystem carbon inputs. Global Change Biology 3:615–623.

Lauenroth, W. K. 1979. Grassland primary production: North American grasslands in perspective. Pages 3–24 *in* N. R. French, editor. Volume 32 of the series Ecological studies, perspectives in grassland ecology. Springer-Verlag, New York, New York, USA.

Lauenroth, W. K. 2013. SGS-LTER standard production data: 1983-2008 annual aboveground net primary production on the central plains experimental range, Nunn, Colorado, USA 1983-2008, ARS Study Number 6. http://hdl.handle.net/10217/81141

Lauenroth, W., and J. Bradford. 2006. Ecohydrology and the partitioning AET between transpiration and evaporation in a semiarid steppe. Ecosystems 5:756–767.

Lauenroth, W. K., I. C. Burke, and M. P. Gutmann. 1999. The structure and function of ecosystems in the central North American grassland region. Great Plains Research 9:223–259.

Lauenroth, W. K., and O. E. Sala. 1992. Long-term forage production of North American shortgrass steppe. Ecological Applications 2:397–403.

Liang, Y. C., J. Y. Yu, M. H. Lo, and C. Wang. 2015. The changing influence of El Niño on the Great Plains low-level jet. Atmospheric Science Letters 16:512–517.

Mantua, N. J., S. R. Hare, Y. Zhang, J. M. Wallace, and R. C. Francis. 1997. A Pacific interdecadal climate oscillation with impacts on salmon production. Bulletin of the American Meteorological Society 78:1069–1079.

McCabe, G. J., and M. D. Dettinger. 1999. Decadal variations in the strength of ENSO teleconnections with precipitation in the western United States. International Journal of Climatology 19:1399–1410.

McCabe, G. J., M. A. Palecki, and J. L. Betancourt. 2004. Pacific and Atlantic Ocean influences on multidecadal drought frequency in the United States. Proceedings of the National Academy of Sciences of the United States of America 101:4136–4141.

Milchunas, D. G., J. R. Forwood, and W. K. Lauenroth. 1994. Productivity of long-term grazing treatments in response to seasonal precipitation. Journal of Range Management 47:133–139.

Morgan, J. A., W. Parton, J. D. Derner, T. G. Gilmanov, and D. P. Smith. 2016. Importance of early season conditions and grazing on carbon dioxide fluxes in Colorado shortgrass steppe. Rangeland Ecology & Management 69:342–350.

Mowll, W., D. M. Blumenthal, K. Cherwin, A. Smith, A. J. Symstad, L. T. Vermeire, S. L. Collins, M. D. Smith, and A. K. Knapp. 2015. Climatic controls of aboveground net primary production in semi-arid grasslands along a latitudinal gradient portend low sensitivity to warming. Oecologia 4:959–969.

National Centers for Environmental Information, NOAA. 2015. Climate data online. http://www.ncdc.noaa.gov/cdo-web/

NOAA [National Oceanic and Atmospheric Administration]. 1992. AVHRR (Advanced Very High Resolution Radiometer) Composites, NASA EOSDIS Land Processes DAAC, USGS Earth Resources Observation and Science (EROS) Center, Sioux Falls, South Dakota. https://doi.org/10.5066/f7707zkn

Parton, W. J. 2013. SGS-LTER standard met data: 1969-2010 manually collected aboveground and belowground meteorological data collected on the central plains experimental range, Nunn, Colorado, USA, ARS Study Number 4. http://hdl.handle.net/10217/82446

Parton, W. J., M. Hartman, D. Ojima, and D. Schimel. 1998. DAYCENT and its land surface submodel: description and testing. Global and Planetary Change 19:35–48.

Parton, W. J., W. K. Lauenroth, and F. M. Smith. 1981. Water loss from a shortgrass steppe. Agricultural Meteorology 24:97–109.

Parton, W., J. Morgan, D. Smith, S. Del Grosso, L. Prihodko, D. Lecain, R. Kelly, and S. Lutz. 2012. Impact of precipitation dynamics on net ecosystem productivity. Global Change Biology 18:915–927.

Physical Sciences Division, ESRL, NOAA. 2015. NCEP reanalysis data (NARR). NOAA/OAR/ESRL PSD, Boulder, Colorado, USA. http://www.esrl.noaa.gov/psd/

Porensky, L. M., J. D. Derner, D. J. Augustine, and D. G. Milchunas. 2017. Plant community composition after 75 yr of sustained grazing intensity treatments in shortgrass steppe. Rangeland Ecology & Management 70:456–464.

Power, S., M. Haylock, R. Colman, and X. Wang. 2006. The predictability of interdecadal changes in ENSO activity and ENSO teleconnections. Journal of Climate 19:4755–4771.

Rangeland Resources Research Unit, ARS. 2015. CPER weather data. http://www.ars.usda.gov/Main/docs.htm?docid=11120

Rayner, N., E. B. Parker, C. K. Horton, L. V. Folland, D. P. Alexander, D. P. Rowell, E. C. Kent, and A. Kaplan. 2003. Global analyses of sea surface temperature, sea ice, and night marine air temperature since the late nineteenth century. Journal of Geophysical Research, 108:4407-1–4407-37.

Reynolds, R. W., T. M. Smith, C. Liu, D. B. Chelton, K. S. Casey, and M. G. Schlax. 2007. Daily high-resolution-blended analyses for sea surface temperature. Journal of Climate 20:5473–5496.

Ritten, J. P., W. M. Frasier, C. T. Bastian, and S. T. Gray. 2010. Optimal rangeland stocking decisions under stochastic and climate-impacted weather. American Journal of Agricultural Economics 92:1242–1255.

Sala, O. E., W. J. Parton, L. A. Joyce, and W. K. Lauenroth. 1988. Primary production of the central grassland region of the United States. Ecology 69:40–45.

Savage, K. E., W. J. Parton, E. A. Davidson, S. E. Trumbore, and S. D. Frey. 2013. Long-term changes in forest carbon under temperature and nitrogen amendments in a temperate northern hardwood forest. Global Change Biology 19:2389–2400.

Scheer, C., S. J. Del Grosso, W. J. Parton, D. W. Rowlings, and P. R. Grace. 2014. Modeling nitrous oxide emissions from irrigated agriculture: testing DayCent with high-frequency measurements. Ecological Applications 24:528–538.

Smith, W. K., S. C. Reed, C. C. Cleveland, A. P. Ballantyne, W. R. Anderegg, W. R. Wieder, Y. Y. Liu, and S. W. Running. 2016. Large divergence of satellite and Earth system model estimates of global terrestrial CO_2 fertilization. Nature Climate Change 6:306–310.

Torell, L. A., S. Murugan, and O. A. Ramirez. 2010. Economics of flexible versus conservative stocking strategies to manage climate variability risk. Rangeland Ecology & Management 63:415–425.

USDA NRCS [U.S. Department of Agriculture, National Water and Climate Center]. 2015. Colorado SCAN Site Nunn #1 (2017) daily weather data. http://www.wcc.nrcs.usda.gov/nwcc/site?sitenum=2017

Wang, S., J. Huang, Y. He, and Y. Guan. 2014. Combined effects of the pacific decadal oscillation and El Nino-Southern Oscillation on global land dry–wet changes. Scientific Reports, 4:6651-1–6651-8.

Yang, L., B. K. Wylie, L. L. Tieszen, and B. C. Reed. 1998. An analysis of relationships among climate forcing and time-integrated NDVI of grasslands over the U.S. Northern and central great plains. Remote Sensing of Environment 1:25–37.

Zhang, Y., J. M. Wallace, and D. S. Battisiti. 1997. ENSO-like interdecadal variability: 1900–1993. Journal of Climate 10:1004–1020.

Zhang, L., B. K. Wylie, L. Ji, T. G. Gilmanov, and L. L. Tieszen. 2010. Climate-driven interannual variability in net ecosystem exchange in the northern Great Plains grasslands. Rangeland Ecology & Management 63:40–50.

Zhu, J., and X. Z. Liang. 2013. Impacts of the Bermuda high on regional climate and ozone over the United States. Journal of Climate 26:1018–1032.

Supporting Information

Additional Supporting Information may be found online at: http://onlinelibrary.wiley.com/doi/10.1002/ecs2.2069/full